



para-Substituted *N*-Nitroso-*N*-oxybenzenamine Ammonium Salts: A New Class of Redox-sensitive Nitric Oxide Releasing Compounds

Andrea D. McGill, Wei Zhang, Joanne Wittbrodt, Jianqiang Wang,
H. Bernhard Schlegel and Peng George Wang*

Department of Chemistry, Wayne State University, Detroit, MI 48202-3489, USA

Received 1 September 1999; accepted 7 November 1999

Abstract—*N*-Nitroso-*N*-oxybenzenamine ammonium salts with -OMe, -Me, -H, -F, -Cl, -CF₃, and -SO₂Me substituents at the *para* position of the phenyl ring constitute a new class of redox sensitive nitric oxide (NO) releasing compounds. These compounds yield nitric oxide and the corresponding nitrosobenzene derivatives by a spontaneous dissociation mechanism after undergoing a one electron oxidation. Oxidation of these compounds can be achieved through chemical, electrochemical and enzymatic methods. It was observed electrochemically that the amount of NO generated was dependent on the substituent effect and the applied oxidation potential. Electron-withdrawing substituents increase the oxidation potential of the compound. A linear correlation was observed when the peak potentials for the oxidation were graphed versus the Hammett substituent constant. Density functional theory calculations were also performed on this series of compounds. The theoretical oxidation energies of the corresponding anions show a strong linear correlation with the experimental potentials. Furthermore, enzymatic oxidation using horseradish peroxidase showed a similar substituent effect. These results indicate that substitution at the *para* position of the phenyl ring has a profound effect on the stability, oxidation potential and enzymatic kinetic properties of the compounds. Thus *para*-substituted *N*-nitroso-*N*-oxybenzenamine salts comprise a new class of redox-sensitive nitric oxide releasing agents. © 2000 Elsevier Science Ltd. All rights reserved.

Introduction

In the past decade, nitric oxide (NO) has been discovered to be a major signaling agent of profound importance throughout the animal kingdom.^{1,2} The major biological functions of NO include controlling blood pressure, smoothing muscle tone and platelet aggregation, assisting the immune system in destroying tumor cells and intracellular pathogens (parasites, virus and bacteria) and participating in neuronal synaptic transmission.^{3–6} Endogenous NO is generated from arginine by the catalytic activity of nitric oxide synthase.^{7,8} Exogenous production from NO releasing agents serves as a valuable tool in biological research for studying the functions of NO and offers a variety of pharmaceutical applications.^{9–12} Thus, the development of new substances and new approaches to the generation of NO is a current challenge facing medicinal and organic chemists.

There are several classes of NO releasing compounds available today (Fig. 1). Different chemical reactions are utilized to generate NO from these compounds. In vivo generation of NO from organic nitrates (e.g. nitroglycerin and isosorbide dinitrate), for example, is believed to occur through thiol-mediated, reductive metabolic pathways.¹³ In vitro generation can occur due to spontaneous and non-spontaneous dissociation mechanisms from NO/nucleophile complexes (NONOates or diazeniumdiolates),^{14–19} sodium nitroprusside,²⁰ *S*-nitrosothiols,^{21–24} sydnonimines,²⁵ and furoxanes.²⁶

Here we report a new class of redox-sensitive NO releasing compounds based on the *N*-nitroso-*N*-oxyarylamine structural moiety.²⁷ The *N*-nitroso-*N*-oxyalkylamine and *N*-nitroso-*N*-oxyarylamine functional groups occur in a variety of natural and synthetic compounds^{28–30} (Fig. 2). Alanosine, a potential antiviral and antitumor drug,^{31,32} and dopastin, a dopamine β -hydroxylase inhibitor,³³ are natural products containing the *N*-nitroso-*N*-oxyalkylamine moiety. The best known member of the synthetic *N*-nitroso-*N*-oxyarylamine family is *N*-nitroso-*N*-oxybenzenamine ammonium salt (cupferron, **3**, Fig. 3) which is commonly used on a large

Keywords: nitric oxide; NO release; *N*-nitroso compound; *N*-nitroso-*N*-oxybenzenamine ammonium salt.

*Corresponding author. Tel.: +1-313-993-6759; fax: +313-577-5831; e-mail: pwang@chem.wayne.edu

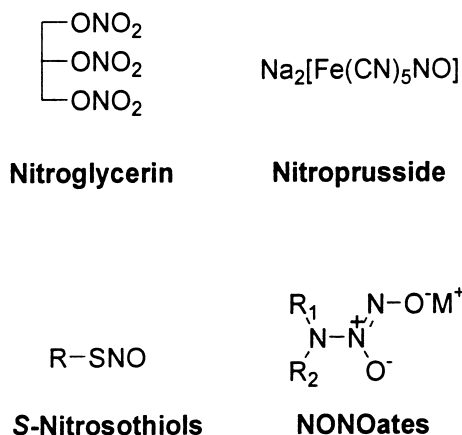


Figure 1. Commonly used NO donor compounds.

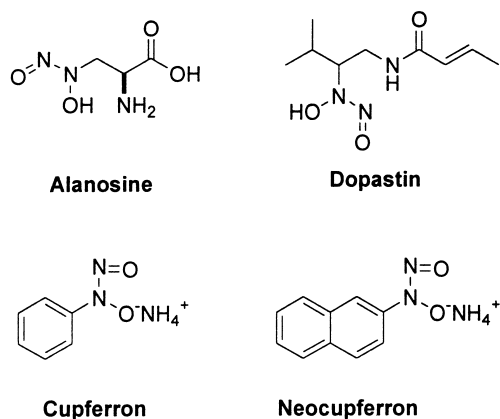


Figure 2. *N*-Nitroso-*N*-oxyalkylamines and *N*-nitroso-*N*-oxyarylamines.

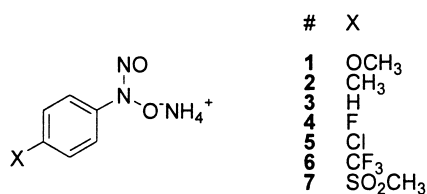


Figure 3. Cupferron, **3**, and the synthetic *para*-substituted ammonium *N*-nitroso-*N*-oxybenzenamines.

scale in industry as a metal chelator³⁴ and as a polymerization inhibitor.^{35,36} The mechanism for the latter effect is related to the thermal dissociation of cupferron to generate NO.³⁷ At room temperature, both in the solid state and in solution, cupferron is relatively stable, generating very little NO. Recently, Balaban and co-workers found that *ortho*-substituted analogues of cupferron have faster decomposition rates due to the substituent preventing the *N*-nitroso-*N*-oxyarylamine from becoming planar.³⁸ They showed that many *ortho*-substituted *N*-nitroso-*N*-oxybenzenamines were good NO donors for both in vitro and in vivo assays. We describe here the generation of NO from the more stable *para*-substituted *N*-nitroso-*N*-oxybenzenamines (Scheme 1). These compounds undergo a one electron oxidation which results in the generation of NO and nitrosobene-

zene. Ab initio calculations were carried out to further study the reaction pathway by providing structural and reaction energy information for the protonated and deprotonated *N*-nitroso-*N*-oxybenzenamines and their radicals.

Results and Discussion

Synthesis of ammonium *N*-nitroso-*N*-oxybenzenamines

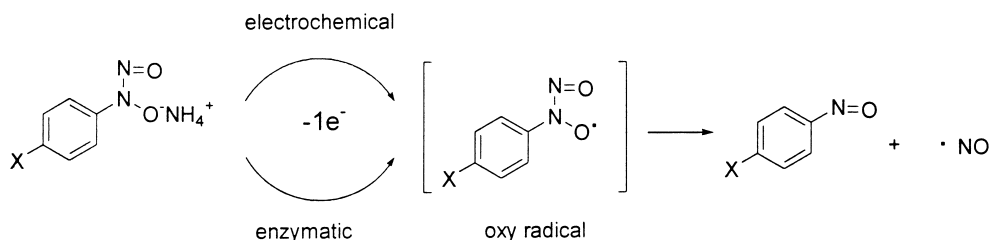
Many methods have been utilized for preparing *N*-nitroso-*N*-oxybenzenamines.^{38–40} In this study, compounds **1–2** and **4–7** (Fig. 3) were synthesized by nitrosation of the corresponding *N*-hydroxyamines, which were readily obtained by reduction of the corresponding nitrobenzenes (Scheme 2).⁴⁰ Products **1–7** are solid and reasonably stable at room temperature. The X-ray crystal structure of ammonium *N*-nitroso-*N*-oxybenzenamine (**3**) was determined and discussed later in comparison with the computational results.

Electrochemical generation of NO

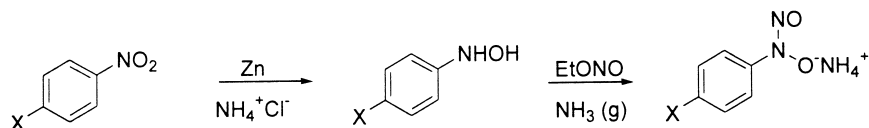
Oxidation of *N*-nitroso-*N*-oxybenzenamine ammonium salts to generate NO can be accomplished enzymatically,⁴¹ electrochemically,^{27,42} chemically (e.g. with lead tetraacetate),⁴³ and thermally and photochemically.⁴⁴ The common intermediate for such oxidations is an *N*-nitrosobenzeneamine-*N*-oxy radical. Balaban and co-workers have prepared some of these *N*-oxy radicals and performed detailed ESR analyses.⁴⁵ In aqueous solution, the radical quickly decomposes to generate a nitric oxide radical and nitrosobenzene. Lawless and co-workers first demonstrated the electrochemical oxidation of cupferron, **3**, while pursuing a method of in situ nitrosobenzene generation.⁴²

We have previously reported the preliminary studies on electrochemical oxidation of *para*-substituted *N*-nitroso-*N*-oxybenzenamine ammonium salts, **1**, **2**, **3**, **5**, **6** and **7**.²⁷ Cyclic voltammetry measurements generated three oxidation peaks (Fig. 4). The first peak corresponds (0.44–0.60 V) to the one-electron oxidation of the *N*-nitroso-*N*-oxybenzenamine to the unstable *N*-nitrosobenzeneamine-*N*-oxy radical intermediate. We found that the substituent on the phenyl ring has a profound effect on the value of this first peak potential. Electron-donating groups lower the oxidation potential, while electron-withdrawing groups have the opposite effect. In fact, a linear correlation exists between the Hammett substituent constants and the first oxidation potential values (Fig. 5). The second and third oxidation peaks in the electrochemical oxidation of the compounds occurred at 0.70 ± 0.04 and 0.82 ± 0.05 V, respectively, which are consistent with the oxidation of NO to nitrite and the oxidation of nitrite to nitrate, respectively.⁴²

To investigate NO release rates and conditions from these compounds, bulk electrolysis^{46–48} was used to generate nitric oxide in solution from the ammonium salts at various controlled potentials while simultaneously measuring the concentration of NO generated



Scheme 1. electrochemical or enzymatic generation of NO from *para*-substituted *N*-nitroso-*N*-oxybenzenamine ammonium salts.



Scheme 2. Synthesis of *para*-substituted *N*-nitroso-*N*-oxybenzenamines.

with a nitric oxide detection apparatus.^{27,49} Within the range of 0.40–0.70 V, the amount of NO generated from compounds 1–7 was influenced by the substituent on the phenyl ring (Table 1). For example, at an applied potential of 0.65 V, the amount of NO generated from the -OMe substituted compound was approximately 20 times the amount generated from the -SO₂Me compound. The concentration of NO generated increased as the applied electrochemical potential increased from around 0.40 to 0.70 V. Above 0.70 V, the concentration of NO decreased as the electrolysis potential increased due to the oxidation of NO. This result was consistent with the cyclic voltammetric data which indicated that a one electron oxidation of NO occurred around 0.70 V to generate nitrite in aqueous solution. To prove this under the conditions of our experiment, gaseous NO was bubbled into an electrolytic solution and the system was then sealed. Once a stable NO concentration was obtained and monitored by the nitric oxide detector, bulk electrolysis was performed while the amount of NO was continually measured, as previously described. As expected, the amount of NO in solution began to decrease only when a potential of 0.70 V or higher was applied.

Enzymatic generation of NO

Horseradish peroxidase has been shown by Alston et al. to be an effective oxidizing enzyme for cupferron and

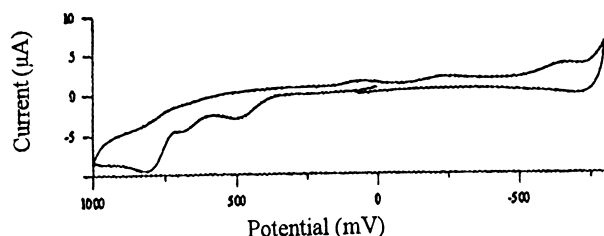


Figure 4. A typical cyclic voltammetry diagram of electrochemical oxidation of compound 1. Measurements were conducted in 0.1 M LiClO₄ solution with 1.33–1.36 mM of compound at pH 7 (adjusted with NH₄OH and HCl solutions). The scan rate was 20 mV/s starting at 0 mV with sweeps in three segments, first oxidatively then reductively then oxidatively.

other compounds with the hydroxynitrosamine moiety.⁴¹ This peroxidase affects a one electron oxidation of the substrate and is regenerated by transferring two electrons to a molecule of H₂O₂. This enzyme is a model for in vivo systems which can oxidize these types of compounds to generate NO. Keefer et al. demonstrated the ability of cupferron to reduce the blood pressure of rats.⁵⁰ Although they did not include stability data, they concluded from Alston's enzymatic oxidation model that NO must be generated from cupferron due to enzymatic processes in their in vivo studies.

The enzymatic oxidation rates of these compounds were also investigated. K_m , k_{cat} and k_{cat}/K_m were determined for compounds 2–4 and 6 by following the formation of the corresponding nitrosobenzene product (Table 2). These compounds were chosen as representatives of the set. Although NO generated by this system was confirmed using the NO-detector, more consistent results were obtained by monitoring nitrosobenzene production by UV–vis techniques. As was evident in the elec-

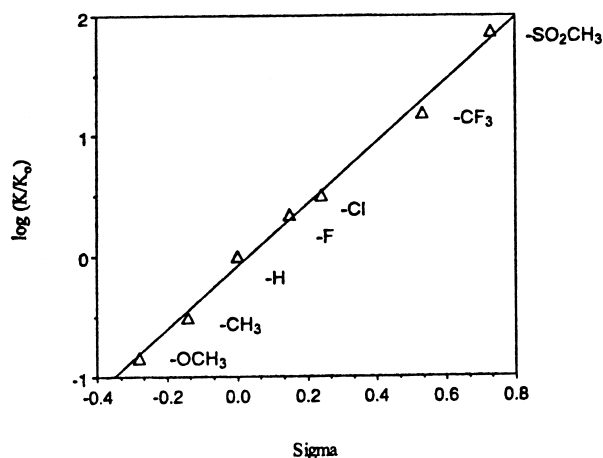


Figure 5. Hammett plot for compounds 1–7. Equilibrium K and K_0 were calculated as $K = e^{(nFE/RT)}$. E , the first oxidation potentials, were obtained by cyclic voltammetry experiments (repeated three times) conducted in 1.3 mM solutions of compounds 1–7 in 0.1 M LiClO₄ at pH 7 (adjusted with NH₄OH and HCl solutions) and at a scan rate of 20 mV/s. $R^2 = 0.995$.

Table 1. Maximum NO concentration generated and applied electrochemical potential for compounds **1**, **3**, **5** and **7**^a

	-OCH ₃ (1)	-H (3)	-Cl (5)	-SO ₂ CH ₃ (7)
Max. concentration (M)	4.6±0.5	4.0±0.4	2.4±0.2	0.6±0.1
Potential (V)	0.65	0.70	0.81	0.75

^aEach experiment was prepared with 1.3 mM of compound in 0.1 M LiClO₄ solution, 12 mL total volume. Electrolysis was conducted at each potential for 5 s intervals. The nitric oxide detector was continuously recording.

Table 2. Rate constant values for the enzymatic oxidation using horseradish peroxidase

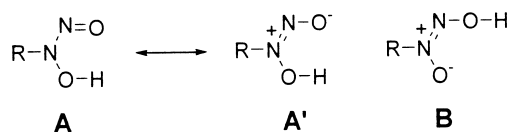
	-CH ₃ (2)	-H (3)	-F (4)	-CF ₃ (6)
<i>k</i> _{cat} (s ⁻¹)	177±9	93.3±5.6	45.5±2.5	5.7±0.4
<i>K</i> _m (mM)	33.3±1.8	65.2±4.3	78.4±5.1	18.4±0.7
<i>k</i> _{cat} / <i>K</i> _m (mM ⁻¹ s ⁻¹)	5.3±0.4	1.4±0.2	0.58±0.07	0.31±0.04

trochemical assay, the rate of the reaction increased with the electron donating effect of the substituent. In the case of **6**, although the *K*_m indicated it bound to the enzyme better than the other three, the rate constant was in line with the substituent effect. The *k*_{cat}/*K*_m values ranged from 0.3 to 5.3 mM⁻¹ s⁻¹, from the most electron withdrawing to the most electron donating substituent. These values indicate that this series of compounds are reasonably good substrates for horseradish peroxidase.

Theoretical calculations

The generation of nitric oxide from *para*-substituted *N*-nitroso-*N*-oxybenzenamine compounds was examined via density functional theory calculations on the following structures: XC₆H₄[N₂O₂]H (two tautomers); the corresponding anion, XC₆H₄[N₂O₂]⁻; radical, XC₆H₄[N₂O₂][•]; and dissociated products, XC₆H₄NO + •NO, for X = OMe, H, F, CF₃ and SO₂Me. For X = H, the transition state (TS) separating the two protonated tautomers was also computed.

There has been some concern over the actual structure of RN₂O₂H containing compounds, for which there are two possible tautomers, **A** and **B** (Fig. 6). In a theoretical study, Hall and co-workers found that tautomer **B** was preferred for a variety of small molecules containing the [N₂O₂]H moiety, including H₂N[N₂O₂]H, Me[N₂O₂]H and H[N₂O₂]H, while for CN[N₂O₂]H a slight preference for **A** was found.⁵¹ Hickmann et al.⁵² have determined that the crystal structure of C₆H₅[N₂O₂]H corresponds to tautomer **B**. Optimized B3LYP/6-31 + G* geometries for both tautomers of

**Figure 6.** Tautomers of RN₂O₂H.

C₆H₅[N₂O₂]H are shown in Figure 7(a) and (b). Both structures are planar about N1 and have significant N1–N2 double bond character. This is similar to the results of Hall and co-workers where, of the various smaller analogues studied, structure **A** was planar about N1 only for ⁻ON₂O₂H, indicating that **A'** is an important resonance contributor when an electron donor is available to stabilize the positive charge on the central nitrogen.⁵¹ Although N1–N2 is longer for tautomer **A** (1.314 Å) than for **B** (1.286 Å), in each case it is longer than a normal N–N double bond (ca. 1.22–1.24 Å)⁵³ but shorter than a single bond (1.4–1.45 Å).

Tautomer **B** is preferred by 1.5 kcal/mol (Table 3) and, taking this as the zero of energy, is separated from tautomer **A** by a transition state at 6.4 kcal/mol. The computed gas phase geometry of **B** agrees well with the solid crystal structure,⁵² the largest error being 1.2% for the N1–O3 bond length. *para*-Substitution with X = OMe, F, CF₃ and SO₂Me has little effect, in terms of both energetics and geometries. For these substituents, tautomer **B** is favored by 0.7 to 2.3 kcal/mol, with bond lengths and angles essentially identical to those of X = H. Calculations on the HN₂O₂H system give similar results, with **B** favored by 2.2 kcal/mol at the B3LYP/6-31 + G* level of theory. This preference is maintained at higher levels of theory. Although the MP2 difference of 6.7 kcal/mol is somewhat larger, the B3LYP result is in good agreement with both the QCISD result of 1.2 kcal/mol and the modified G2 result of 3.9 kcal/mol, thus indicating the reliability of the B3LYP results for XC₆H₄N₂O₂H.

The cupferron anion, which can be formed by proton loss from either tautomer **A** or **B**, is shown in Figure 7(c). This structure is a hybrid of the protonated geometries, but is more like **A** as evidenced by the similar N2–O4 and N1–C5 bond lengths. The computed gas phase

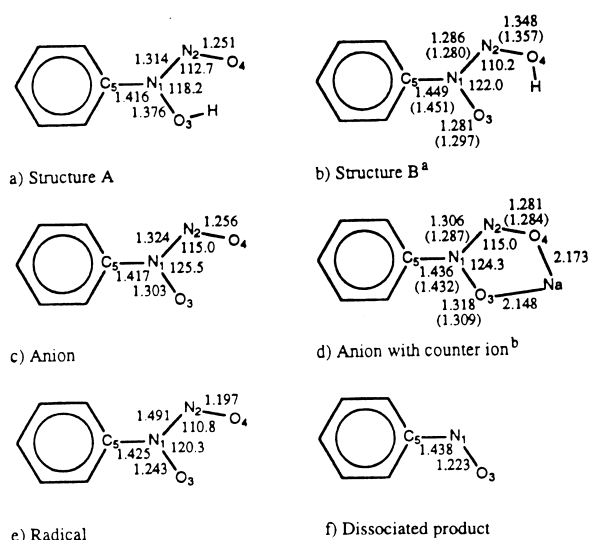
**Figure 7.** B3LYP/6-31 + G* optimized structures for X = H. ^aNumbers in parentheses for tautomer **B** correspond to the crystal structure of Hickmann et al.⁵² ^bNumbers in parentheses for anion with counter ion correspond to the cupferron crystal structure. Bond lengths are in angstroms, angles are in degrees.

Table 3. Relative energetics for $\text{XC}_6\text{H}_4\text{N}_2\text{O}_2\text{H}$ and $\text{HN}_2\text{O}_2\text{H}^{\text{a}}$

$\text{XC}_6\text{H}_4\text{N}_2\text{O}_2\text{H}$	Tautomerization energy A–B	Proton affinity anion–B	Oxidation energy Radical–anion	Dissociation energy RNO+NO–radical
X = OCH_3	2.34	344.67	51.44	6.30
H	1.51	342.07	54.45	7.27
F	1.83	339.23	57.31	6.47
CF_3	2.14	333.44	64.44	7.63
SO_2CH_3	0.70	329.18	67.44	7.79
$\text{HN}_2\text{O}_2\text{H}$				
B3LYP	2.20	346.45	51.86	14.14
MP2 ^b	6.75	346.58		
QCISD ^c	1.17	357.56	40.19	–0.72
Mod. G2 ^d	3.89	353.99	54.31	3.89

^aIn kcal/mol at the B3LYP/6-31 + G* level of theory unless otherwise noted. See Figure 7 for selected structures.

^bMP2/6-31 + G* optimized. Spin contamination problems were encountered for the radicals.

^cQCISD/6-311 + G** optimized.

^dG2 single point corrections on the B3LYP/6-31 + G* optimized geometry.

anion geometry shows significant errors when compared to the crystal structure of cupferron, with the N1–N2 bond 4% longer and the N2–O4 bond 2% shorter. Including Na^+ as a counter ion in the calculation (Fig. 7(d)) reduces the N1–N2 error to 1.5% while the other bonds are in error by less than 1%. The geometries of the X = OMe and F anions are almost identical to the X = H geometry, while for X = CF_3 and SO_2Me , N1–N2 is 0.014–0.019 Å longer, N2–O4 is 0.008–0.011 Å shorter, N1–O3 is 0.005–0.007 Å shorter, and N1–C5 is 0.012–0.015 Å shorter. The proton affinities of these substituted *N*-nitroso-*N*-oxybenzenamine anions range from 345 to 329 kcal/mol, decreasing as the electron withdrawing ability of the substituent increases (Table 3). These data show a linear correlation ($R^2 = 0.974$) when plotted against the Hammett substituent constants.

For each anion, oxidation to the corresponding radical (Fig. 7(e)) causes N1–N2 to lengthen by ca. 0.15 Å and N2–O4 to shorten by ca. 0.06 Å. The energy required for oxidation correlates well with both the substituent constants (Fig. 8) and the experimental oxidation potentials (Fig. 9). The radicals then easily dissociate to form RNO + NO with the products 6–8 kcal/mol higher in energy at the B3LYP/6-31 + G* level of theory. The dissociation energies do not appear to have any

correlation with the substituent constants. For HN_2O_2 , the dissociation energy is larger, ca. 14 kcal/mol at the B3LYP/6-31 + G* level of theory. (Although we were unable to find a transition state for this dissociation, calculations at the same level of theory suggest that if a TS exists, it is probably less than 2 kcal/mol higher in energy than the products.) Higher level calculations on this system indicate that the energy difference may disappear, or is much smaller (Table 3). At the QCISD/6-311 + G** level of theory the dissociation energy is slightly negative. However, this method is susceptible to spin contamination problems that typically are not encountered in the G2 method, which gives a dissociation energy of 4 kcal/mol. Thus it is shown that oxidation of the anion is the key step in the release of nitric oxide.

Conclusions

para-Substituted *N*-nitroso-*N*-oxybenzenamine ammonium salts constitute a library of redox-sensitive NO donor compounds, which generate NO electrochemically at well-defined electrolysis potentials. More importantly, these potentials are in the window of nitric

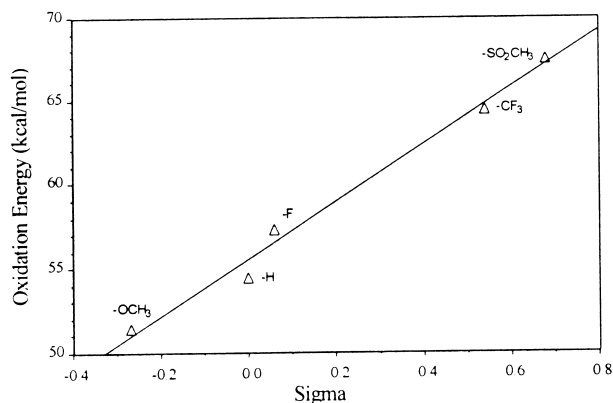


Figure 8. B3LYP/6-31 + G* oxidation energy of the anions versus the Hammett substituent constants. $R^2 = 0.988$.

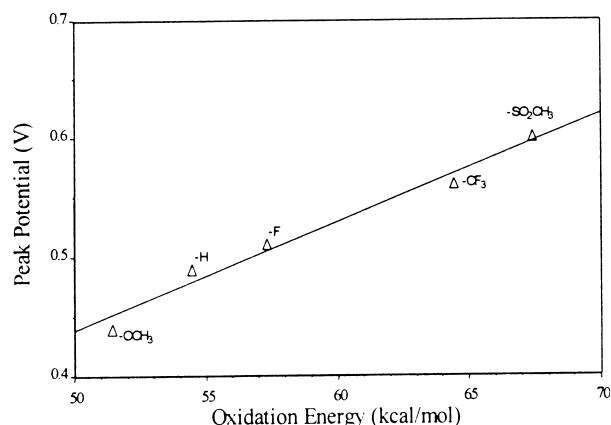


Figure 9. Experimental oxidation potential versus the B3LYP/6-31 + G* oxidation energy. $R^2 = 0.975$.

oxide generation without oxidation of the nitric oxide. It has been shown that the rate of NO release can be modified by varying the *para*-substituent under appropriate oxidation conditions. *para*-Substitution has a similar effect on the enzymatic oxidation rate when assayed versus horseradish peroxidase. Theoretical calculations are in good agreement with the experimental results as shown by the linear correlation between the computational oxidation energies of the anions and the experimental oxidation potentials.

Such a redox controlled electrochemical NO generating system has potential for use in a variety of biomedical applications. The biological activity and toxicity studies are currently in progress to further evaluate this new class of NO-donating compounds.

Experimental

General

¹H NMR and ¹³C NMR spectra were recorded on a Varian Mercury 300 MHz or Varian Mercury 400 MHz spectrometer. Silica gel plates (Merck F₂₅₄) were used for thin-layer chromatography (TLC). Elemental analyses were performed at Atlantic Microlab. UV-vis spectra were obtained with a Milton-Roy, Genesys 2 spectrophotometer. Kinetic data were obtained with the use of an HP 8453 UV-visible spectrophotometer. Compound **3** was obtained from Wako Pure Chemical Industries, Ltd., Osaka, Japan.

General procedure for the synthesis of *para*-substituted *N*-nitroso-*N*-oxybenzenamine ammonium salts

Compounds **1–2** and **4–7** were prepared by nitrosating the corresponding *N*-hydroxyamine compounds, which were obtained from the reduction of the corresponding nitrobenzenes.⁴⁰ Zinc dust (1.5 equiv) was added to a stirring solution (water:methanol, 1:5; v:v) of ammonium chloride (1.5 equiv) and the corresponding nitrobenzene (1 equiv) at 0 °C. The reactions were monitored by TLC methods and excess ammonium chloride and zinc dust were added as needed until the starting material was depleted, or the reaction began to yield byproducts. The solution was then filtered and the filtrate was again brought to 0 °C. (For compounds **4** and **6**, the solvent was evaporated after filtration and the product was dissolved in ether.) Ammonia gas was bubbled through the solution and after 15 min ethyl nitrite (1.2 equiv) was added (isoamyl nitrite for compounds **4** and **6**). When the reaction was complete, the product was allowed to crystallize slowly in solution over several hours at –20 °C. The product was collected by vacuum filtration and rinsed with methylene chloride. Additional product was collected from the filtrate by rotary evaporation to dryness (without heating) followed by recrystallization in ethyl acetate.

***N*-Nitroso-*N*-oxy-*p*-methoxybenzenamine ammonium salt (1).** Synthesized from 4-nitroanisole (3%) as a light-brown solid: ¹H NMR (CD₃OD, 300 MHz) δ 3.82 (3H,

s, OCH₃), 6.96 (2H, d, ar), 7.81 (2H, d, ar); ¹³C NMR (CD₃OD) δ 120.44, 113.38, 54.58. UV-vis λ_{max} 283 nm. Anal. calcd for C₇H₁₁N₃O₃: C, 45.41; H, 5.99; N, 22.70. Found: C, 45.17; H, 5.78; N, 22.46. It is necessary to store compound **1** at –78 °C since decomposition begins to occur overnight at room temperature or in a few weeks at –20 °C.

***p*-Amino-*N*-nitroso-*N*-oxytoluene ammonium salt (2).** Synthesized from 4-nitrotoluene (44%) as a pale-yellow solid: ¹H NMR (CD₃OD, 300 MHz) δ 2.37 (3H, s, CH₃), 7.26 (2H, d, ar), 7.82 (2H, d, ar); ¹³C NMR (CD₃OD) δ 130.25, 120.37, 21.02; UV-vis λ_{max} 283 nm. Anal. calcd for C₇H₁₁N₃O₂: C, 49.69; H, 6.55; N, 24.85. Found: C, 49.66; H, 6.51; N, 24.79.

***N*-Nitroso-*N*-oxy-*p*-fluorobenzenamine ammonium salt (4).** Synthesized from 1-fluoro-4-nitrobenzene (40%) as a white solid: ¹H NMR (CD₃OD, 400MHz) δ 7.52 (2H, t, ar), 8.18 (2H, t, ar); ¹³C NMR (CD₃OD) δ 120.61, 114.95, 114.65, 103.47; UV-vis λ_{max} 283 nm. Anal. calcd for C₆H₈FN₃O₂: C, 41.62; H, 4.66. Found: C, 41.71; H, 4.61.

***N*-Nitroso-*N*-oxy-*p*-chlorobenzenamine ammonium salt (5).** Synthesized from 1-chloro-4-nitrobenzene (54%) as a white solid: ¹H NMR (CD₃OD, 400 MHz) δ 7.31 (2H, d, ar), 7.80 (2H, d, ar); ¹³C NMR (CD₃OD, 300 MHz) δ 128.23, 119.99; UV-vis λ_{max} 300 nm. Anal. calcd for C₆H₈ClN₃O₂: C, 37.98; H, 4.22; N, 22.16; Cl, 18.73. Found: C, 38.00; H, 4.26; N, 22.07; Cl, 18.61.

***p*-Amino-*N*-nitroso-*N*-oxy- α,α,α -trifluorotoluene ammonium salt (6).** Synthesized from 4-nitro- α,α,α -trifluorotoluene (37%) as a light-yellow solid: ¹H NMR (CD₃OD, 300 MHz) δ 7.72 (2H, d, ar), 8.11 (2H, d, ar); ¹³C NMR (CD₃OD, 300 MHz) δ 125.50, 118.74; UV-vis λ_{max} 298 nm. Anal. calcd for C₇H₈F₃N₃O₂: C, 37.67; H, 3.61. Found: C, 37.39; H, 3.65.

Methyl *p*-nitrophenylsulphone. Methyl 4-nitrophenyl sulfide (2.54, 0.015 mol) was dissolved in 60 mL of acetone. H₂O₂ (10 mL) was added and the reaction was heated to 60 °C. After stirring for 30 min, two more equivalents of H₂O₂ (10 mL) were added and the reaction was stirred for 2 h. Most of the solvent was removed through rotary evaporation. The residue was extracted with CHCl₃. The organic phase was dried over MgSO₄, filtered and then concentrated. The product was isolated by column chromatography (silica gel, hexane:ethyl acetate; 1:1 then 1:2) as a pale-yellow solid (23%): mp: 102.0–104.5 °C; ¹H NMR (CDCl₃, 400 MHz) δ 3.14 (3H, s, CH₃), 8.18 (2H, d, ar), 8.43 (2H, d, ar); MS (*m/e*): 201 (M⁺, 53), 186 (44), 139 (100), 122 (36), 109 (18), 92 (14), 76 (16), 63 (17).

***N*-Nitroso-*N*-oxy-*p*-methylsulfonylbenzenamine ammonium salt (7).** Synthesized from methyl *p*-nitrophenylsulphone (42%) as a white, crystalline solid: ¹H NMR (400 MHz, CD₃OD) δ 2.05 (s, 3H, CH₃), 3.05 (s), 7.91 (d, 2H, ar), 8.09 (d, 2H, ar); UV-vis λ_{max} 321 nm. Anal. calcd for C₇H₁₁N₃O₄S: C, 36.05; H, 4.72; N, 18.03; S 13.73. Found: C, 36.09; H, 4.70; N, 17.87; S, 13.64.

Stability measurement of *N*-nitroso-*N*-oxybenzenamines.

A solution of each compound 1–7 was prepared in sodium phosphate buffer (50 mM, pH 7.4). The concentration of each solution was adjusted in order to achieve an absorption of 1–2 at the corresponding maximum wavelength. The stability of the solution was observed by following the absorption over time.

Electrochemical measurements. A platinum working electrode, 1.6 mm in diameter (from Bioanalytical Systems (BAS), West Lafayette, IN), a platinum wire counter electrode (BAS), and a Ag/AgCl reference electrode (BAS) were employed in all cyclic voltammetry measurements. Working and counter platinum gauze electrodes, 13×13 mm (160 mm² surface area) flag-like in shape, were used in all electrolysis experiments. (These electrodes were made by annealing platinum mesh onto platinum wire. The metals were obtained from Fisher Scientific, Pittsburgh, PA.) The supporting electrolyte, LiClO₄, was recrystallized in ethanol, and dried under vacuum. Doubly distilled water was used as the solvent. In each case, the solution was argonated before each experiment and measurements were performed under an argon atmosphere. Cyclic voltammograms were recorded at 20 mV/s and all measurements were performed at room temperature. An airtight, dual chamber electrochemical cell was glass blown in house.^{46–48} An inlet was made for each of the electrodes and NO detector probe as well as for the argon tubes. An airtight seal was assured by using o-rings and inlet caps. Clamps were used to enhance the fit of the cell caps. Electrolysis was conducted using the BAS 100W program to operate the BAS 100B electrochemical analyzer.

NO measurements. NO concentration measurements were conducted using an ISO-NOP 2 mm electrode probe, ISO-NOP Mark II meter and data collected using the DUO.18 software from World Precision Instruments, Inc. (Sarasota, FL).

Electrolysis and NO concentration measurements. Each experiment was run with 1.35 mM of compound in 0.1 M LiClO₄ solution. Electrolysis was conducted at each potential ranging from 0.25 to 1.00 V at 0.05 V increments. The nitric oxide detector was continuously recording. Once the baseline current of the NO detector was constant, a potential was applied to the system for 5 s with constant stirring at 1100 rpm. Once the concentration peak of the NO detector stabilized again to a constant value, the baseline current was subtracted from the NO peak (or plateau) value in order to determine the amount of NO generated. Key values are listed in Table 2. Five seconds was enough time to minimize experimental error and achieve reproducible results. A longer time period would only aid in exhausting the starting material in solution, thus adding equilibrium shift errors into the measurement. Also, the computer program driven meter only records up to 4.8 μM of nitric oxide before it gets saturated. The total amount of NO generated in each experiment was well below the solubility limit of NO in solution.

Theoretical calculations. Geometries were fully optimized in redundant cartesian coordinates and energies computed at the B3LYP/6-31+G* level of theory⁵⁴ using the Gaussian94⁵⁵ series of programs. The B3LYP method was chosen because it includes electron correlation, yet is less expensive than MP2 and exhibits less spin contamination for radicals as well. To assess the accuracy of these results, structures in the HN₂O₂H system were optimized at several levels of theory; B3LYP/6-31+G*, MP2/6-31+G* and QCISD/6-311+G**.⁵⁶ Furthermore, approximate QCISD(T)/6-311+G(3df,2p) energetics were computed for the B3LYP structures using the single point corrections of the high accuracy G2 method.⁵⁷ (The other portions of this method, zero point and empirical corrections, were not included.) To verify the nature of the final geometries, frequency calculations were performed for all of the B3LYP and MP2 optimized HN₂O₂H structures. Due to the size of the larger XC₆H₄N₂O₂H systems, frequencies were computed only for the two protonated structures and the associated TS of X=H.

Enzymatic assay. A stock solution of 1.13 mM horseradish peroxidase was prepared in 50 mM sodium phosphate buffer (pH 7.4) containing 1 mM EDTA. Stock solutions for each compound were prepared by making a saturated sodium phosphate solution of the compound. A stock solution of H₂O₂ was prepared, adjusting the concentration with water to match the concentration of the respective compound. In kinetic measurements, the formation of the *para*-substituted nitrosobenzene from 3.6 to 68.3 mM of the *para*-substituted *N*-nitroso-*N*-oxybenzenamines and equal amounts of H₂O₂ with 0.1–4.6 μM horseradish peroxidase was monitored by UV–vis at 365 nm for compounds 2 and 3, 351 nm for compound 4 and 254 nm for compound 6. *K*_m and *k*_{cat} values were calculated from a Lineweaver–Burk plot for each compound.

Acknowledgments

This work was supported by the NIH (GM54074) and American Heart Association, Florida Affiliation. Andrea McGill thanks the National Science Foundation for support through her predoctoral fellowship. Thanks are also due to Dr. Petersen for the use of his electrochemical equipment, to David Daenzer for constructing the electrochemical cell, and to Mary Jane Heeg for elucidation of the crystal structure of cupferron.

References and Notes

1. Kerwin, Jr., J. F.; Lancaster, Jr., J. R.; Feldman, P. L. *J. Med. Chem.* **1995**, *38*, 4343.
2. Williams, R. J. P. *Chem. Soc. Rev.*, **1996**, 77.
3. Moncada, S.; Palmer, R. M. J.; Higgs, E. A. *Pharmacol. Rev.* **1991**, *43*, 109.
4. Bredt, D. S.; Snyder, S. H. *Annu. Rev. Biochem.* **1994**, *63*, 175.

5. Schmidt, H. H. W.; Walter, U. *Cell* **1994**, 78, 919.
6. Feldman, P. L.; Griffith, O. W.; Stuehr, D. J. *Chem. & Eng. News* **1993**, 71 (20 December), 26.
7. Nathan, C.; Xie, Q.-W. *Cell* **1994**, 78, 915.
8. Marletta, M. A. *Cell* **1994**, 78, 927.
9. Hanson, S. R.; Hutsell, T. C.; Keefer, L. K.; Mooradian, D. L.; Smith, D. J. In *Nitric Oxide: Biochemistry, Molecular Biology and Therapeutic Implications*; Ignarro, L.; Murad, F., Eds.; Academic Press: San Diego, 1995; p 383.
10. Guo, Z.-M.; McGill, A.; Yu, L.-B.; Li, J.; Ramirez, J.; Wang, P. G. *Bioorg. Med. Chem. Lett.* **1996**, 6, 573.
11. Yu, L.-B.; McGill, A.; Ramirez, J.; Wang, P. G.; Zhang, Z. *Y. Bioorg. Med. Chem. Lett.* **1995**, 5, 1003.
12. Ramirez, J.; Yu, L.-B.; Li, J.; Braunschweiger, P. G.; Wang, P. G. *Bioorg. Med. Chem. Lett.* **1996**, 6, 2575.
13. Bauer, J. A.; Booth, B. P.; Fung, H.-L. In *Nitric Oxide: Biochemistry, Molecular Biology and Therapeutic Implications*; Ignarro, L.; Murad, F., Eds.; Academic Press: San Diego, 1995; p 361.
14. Morley, D.; Keefer, L. K. *J. Cardiovasc. Pharmacol.* **1993**, 22 (Suppl. 7), S3.
15. Saavedra, J. E.; Dunams, T. M.; Flippen-Anderson, J. L.; Keefer, L. K. *J. Org. Chem.* **1992**, 57, 6134.
16. Hrabie, J. A.; Klose, J. R.; Wink, D. A.; Keefer, L. K. *J. Org. Chem.* **1993**, 58, 1472.
17. Smith, D. J.; Chakravarthy, D.; Pulfer, S.; Simmons, M. L.; Hrabie, J. A.; Citro, M. L.; Saavedra, J. E.; Davies, K. M.; Hutsell, T. C.; Mooradian, D. L.; Hanson, S. R.; Keefer, L. K. *J. Med. Chem.* **1996**, 39, 1148.
18. Saavedra, J. E.; Southan, G. L.; Davies, K. M.; Lundell, A.; Markou, C.; Hanson, S. R.; Adrie, C.; Hurford, W. E.; Zapol, W. M.; Keefer, L. K. *J. Med. Chem.* **1996**, 39, 4361.
19. Keefer, L. K. *Chemtech.* **1998**, 8, 30.
20. Richter-Addo, G. B.; Legzdins, P. *Metal Nitrosyls*; Oxford University Press: New York, 1992.
21. Stamler, J. S.; Singel, D. J.; Loscalzo, J. *Science* **1992**, 258, 1898.
22. Stamler, J. S. *Cell* **1994**, 78, 931–936.
23. Stamler, J. S. *Current Topics in Microbiology and Immunology*; Koprowski, H.; Maeda, H., Eds.; Springer-Verlag: New York, 1995; p 19.
24. Williams, D. L. H. *Chem. Soc. Rev.* **1985**, 14, 171.
25. Feelisch, M.; Ostrowski, J.; Noack, E. *J. Cardiovasc. Pharmacol.* **1989**, 14, S13.
26. Medana, C.; Ermondi, G.; Fruttero, R.; Di Stilo, A.; Ferretti, C.; Gasco, A. *J. Med. Chem.* **1994**, 37, 4412.
27. McGill, A. D.; Yang, Y.; Wang, J.; Echegoyen, L.; Wang, P. G. In *Methods in Enzymology*; Packer, L., Ed.; Academic Press: CA, 1998; Vol. 301, Chapter 25, p. 235.
28. Kano, K.; Anselme, J.-P. *Tetrahedron.* **1993**, 49, 9453.
29. Kano, K.; Anselme, J.-P. *J. Org. Chem.* **1993**, 58, 1564.
30. Kano, K.; Anselme, J.-P. *Tetrahedron.* **1992**, 48, 10075.
31. Murthy, Y. K. S.; Thiemann, J. E.; Coronelli, C.; Sensi, P. *Nature* **1966**, 211, 1198.
32. Fumarola, D. *Pharmacology* **1970**, 3, 215.
33. Inuma, H.; Takeuchi, T.; Kondo, S.; Matsuzaki, H.; Umezawa, H.; Ohno, M. *J. Antibiot.* **1972**, 25, 497.
34. Paneli, M.; Ouguenoune, H.; David, F.; Bolyos, A. *Anal. Chim. Acta.* **1995**, 304, 177.
35. Scates, M. O.; Dougherty, E. F. European Patent, 0 301 879 A2, 1989.
36. Ulbricht, J.; Hoering, S. *Plaste Kaut.* **1968**, 15, 396.
37. Kende, I.; Sumegi, L.; Tudos, F. *Polymer Bulletin.* **1980**, 3, 325.
38. Garfield, R. E.; Balaban, A. T.; Seitz, W. A.; Klein, D. J.; Lesko, M. International Patent, WO 96/36326, 1996.
39. George, M. V.; Kierstead, R. W.; Wright, G. F. *Can. J. Chem.* **1959**, 37, 679.
40. Balaban, A. T.; Garfield, R. E.; Lesko, M. J.; Seitz, W. A. *Org. Prep. Proced. Int.* **1998**, 30, 439.
41. Alston, T. A.; Porter, D. J. T.; Bright, H. J. *J. Biol. Chem.* **1985**, 260, 4069.
42. Lawless, J. G.; Hawley, M. D. *Electrochemical Oxidation of Cupferron Anal. Chem.* **1968**, 40, 948.
43. Balaban, A. T.; Negoita, N.; Pascaru, I. *Rev. Roum. Chim.* **1971**, 16, 721.
44. Hwu, J. R.; Yau, C. S.; Tsay, S.-C.; Ho, T.-I. *Tetrahedron Lett.* **1997**, 38, 9001.
45. Balaban, A. T.; Negoita, N.; Baican, R. *J. Mag. Res.* **1973**, 9, 1.
46. Fry, A. *Synthetic Organic Electrochemistry*; 2nd ed.; Wiley: New York, 1989.
47. Bard, A. J.; Faulkner, L. R. *Electrochemical Methods: Fundamentals and Applications*. Wiley: New York, 1980.
48. Kaifer, A. E. In *Comprehensive Supramolecular Chemistry*; Davies, J. E. D., Ed.; Elsevier Science: London, 1996; Vol. 8, p 499.
49. The electrochemical cell was designed with an airtight seal modeled from: Rasmussen, S. C.; Richter, M. M.; Yi, E.; Place, H.; Brewer, K. J. *Inorg. Chem.* **1990**, 29, 3926.
50. Keefer, L.; Wink, D. A.; Dunams, T. M.; Hrabie, J. A. US Patent, 5,212,204, 1993.
51. Taylor, D. K.; Bytheway, I.; Barton, D. J. R.; Bayse, C. A.; Hall, M. B. *J. Org. Chem.* **1995**, 60, 435.
52. Hickmann, E.; Hadicke, E. and Reuther, W. *Tetrahedron Lett.* 2457, 1979.
53. Allen, F. H.; Kennard, O.; Watson, D. G.; Brammer, L.; Orpen, A. G.; Taylor, R. *J. Chem. Soc. Perkin Trans. 2* **1987**, S1.
54. Becke, A. D. *J. Chem. Phys.* **1993**, 98, 5648.
55. Frisch, M. J.; Trucks, G. W.; Schlegel, H. B.; Gill, P. M. W.; Johnson, B. G.; Robb, M. A.; Cheeseman, J. R.; Keith, T. A.; Petersson, G. A.; Montgomery, J. A.; Raghavachari, K.; Al-Laham, M. A.; Zakrzewski, V. G.; Ortiz, J. V.; Foresman, J. B.; Peng, C. Y.; Ayala, P. Y.; Wong, M. W.; Andres, J. L.; Replogle, E. S.; Gomperts, R.; Martin, R. L.; Fox, D. J.; Binkley, J. S.; Defrees, D. J.; Baker, J.; Stewart, J. P.; Head-Gordon, M.; Gonzalez, C.; Pople, J. A. *Gaussian 94* (Revision C.3); Gaussian: Pittsburgh, PA, 1995.
56. Pople, J. A.; Head-Gordon, M.; Raghavachari, K. *J. Chem. Phys.* **1987**, 87, 5968.
57. Curtiss, L. A.; Raghavachari, K.; Trucks, G. W.; Pople, J. A. *J. Chem. Phys.* **1991**, 94, 7221.